ORIGINAL ARTICLE

Journal of Cachexia, Sarcopenia and Muscle 2019; **10**: 630–642
Published online 20 March 2019 in Wiley Online Library (wileyonlinelibrary.com) **DOI:** 10.1002/jcsm.12409

Fibroblast growth factor 21 controls mitophagy and muscle mass

Lynette J. Oost[1,2], Monika Kustermann[1,3], Andrea Armani[1,4], Bert Blaauw[1,4,5] & Vanina Romanello[1,4,5,*]

[1]*Venetian Institute of Molecular Medicine, Padova, Italy,* [2]*Minderbroedersberg, Maastricht, LK, The Netherlands,* [3]*Molecular Cardiology, Department of Internal Medicine II, University of Ulm, Ulm, Germany,* [4]*Department of Biomedical Sciences, University of Padova, Padova, Italy,* [5]*Myology Center, Department of Biomedical Science, University of Padova, Padova, Italy*

Abstract

Background Skeletal muscle is a plastic tissue that adapts to changes in exercise, nutrition, and stress by secreting myokines and myometabolites. These muscle-secreted factors have autocrine, paracrine, and endocrine effects, contributing to whole body homeostasis. Muscle dysfunction in aging sarcopenia, cancer cachexia, and diabetes is tightly correlated with the disruption of the physiological homeostasis at the whole body level. The expression levels of the myokine fibroblast growth factor 21 (FGF21) are very low in normal healthy muscles. However, fasting, ER stress, mitochondrial myopathies, and metabolic disorders induce its release from muscles. Although our understanding of the systemic effects of muscle-derived FGF21 is exponentially increasing, the direct contribution of FGF21 to muscle function has not been investigated yet.

Methods Muscle-specific FGF21 knockout mice were generated to investigate the consequences of FGF21 deletion concerning skeletal muscle mass and force. To identify the mechanisms underlying FGF21-dependent adaptations in skeletal muscle during starvation, the study was performed on muscles collected from both fed and fasted adult mice. *In vivo* overexpression of FGF21 was performed in skeletal muscle to assess whether FGF21 is sufficient *per se* to induce muscle atrophy.

Results We show that FGF21 does not contribute to muscle homeostasis in basal conditions in terms of fibre type distribution, fibre size, and muscle force. In contrast, FGF21 is required for fasting-induced muscle atrophy and weakness. The mass of isolated muscles from control-fasted mice was reduced by 15–25% ($P < 0.05$) compared with fed control mice. FGF21-null muscles, however, were significantly protected from muscle loss and weakness during fasting. Such important protection is due to the maintenance of protein synthesis rate in knockout muscles during fasting compared with a 70% reduction in control-fasted muscles ($P < 0.01$), together with a significant reduction of the mitophagy flux via the regulation of the mitochondrial protein Bnip3. The contribution of FGF21 to the atrophy programme was supported by *in vivo* FGF21 overexpression in muscles, which was sufficient to induce autophagy and muscle loss by 15% ($P < 0.05$). Bnip3 inhibition protected against FGF21-dependent muscle wasting in adult animals ($P < 0.05$).

Conclusions FGF21 is a novel player in the regulation of muscle mass that requires the mitophagy protein Bnip3.

Keywords FGF21; Myokine; Mitophagy; Autophagy; Muscle atrophy; Bnip3

Received: 28 August 2018; Revised: 12 December 2018; Accepted: 17 January 2019
**Correspondence to:Vanina Romanello, Venetian Institute of Molecular Medicine, via Orus 2, Padova 35129, Italy. Email: vanina.romanello@unipd.it*

Introduction

Loss of muscle function has major implications for human health because it can lead to reduced quality of life, increased morbidity, and mortality. In humans, muscle strength decline is the best predictor of the risk of developing several chronic diseases and of mortality.[1] In fact, muscle atrophy and weakness occur in several systemic conditions such as starvation, aging sarcopenia, mitochondrial myopathies, and cancer cachexia.[2] Moreover, alterations in muscle homeostasis can be reflected at the whole body level. Exercise, nutritional changes, organelle dysfunction, and stress induce the

© 2019 The Authors. Journal of Cachexia, Sarcopenia and Muscle published by John Wiley & Sons Ltd on behalf of the Society on Sarcopenia, Cachexia and Wasting Disorders
This is an open access article under the terms of the Creative Commons Attribution-NonCommercial-NoDerivs License, which permits use and distribution in any medium, provided the original work is properly cited, the use is non-commercial and no modifications or adaptations are made.

systemic release of muscle-derived factors: cytokines (myokines) and metabolites (myometabolites) that exert autocrine, paracrine, or endocrine effects.[3–5] Indeed, exercise preserves and ameliorates mitochondrial function and muscle metabolism, thereby affecting the release of myokines and metabolites, which might systemically counteract organ deterioration. In contrast, dysfunctional muscles can influence disease progression in other tissues.[3,4] The fibroblast growth factor 21 (FGF21) is a secreting myokine[6] that can also be released in the bloodstream by other organs such as liver,[7,8] heart,[9] white adipose tissue[10] (WAT), and brown adipose tissue (BAT).[11] It is a starvation-like hormone with several metabolic functions aimed at overcoming nutrient deprivation by providing tissues with fuel. In skeletal muscle, FGF21 expression, in healthy conditions, is almost undetectable, and therefore, the circulating FGF21 is predominantly produced and released by the liver.[6,12] In contrast, muscle-dependent systemic release of FGF21 increases with starvation, endoplasmic reticulum stress, mitochondrial dysfunction, obesity, mitochondrial myopathies, and aging.[6,13–19] Moreover, FGF21 is a stress-induced myokine that has been proposed as a specific serum biomarker of muscle-specific mitochondrial disorders.[17,20] Moreover, we and others recently demonstrated that in a muscle-specific OPA1 knockout animal model, characterized by mitochondrial dysfunction and by extensive muscle loss, the contribution of skeletal muscle to circulating FGF21 was predominant.[15,16,18] In this model, FGF21 secreted from muscles mediates an integrated stress response that caused several systemic cell non-autonomous effects such as inflammation, metabolic alterations, and precocious senescence.[18] In agreement, a positive correlation of serum FGF21 levels and aging-sarcopenia has been found.[18,21] Importantly, FGF21 deletion in OPA1 knockout muscles improved almost all systemic effects, while there was only a partial sparing of muscle mass.[18] Injecting mice daily with exogenous FGF19, a closely related endocrine FGF member produced in the gut, increased skeletal muscle mass and strength. Remarkably, the skeletal muscle hypertrophy effects were not elicited by administrating FGF21.[22] Thus, whether FGF21 is beneficial or detrimental for human health is still not clear, in part because the contribution of autocrine/paracrine-derived FGF21 signalling to muscle homeostasis has not been investigated yet. Here, we aim to study, *in vivo*, the functional role of FGF21 in skeletal muscle.

Materials and methods

Animal handling and generation of muscle-specific fibroblast growth factor 21 knockout mice

Animals were handled by specialized personnel under the control of inspectors of the Veterinary Service of the Local Sanitary Service (ASL 16—Padova), the local officers of the Ministry of Health. All procedures are specified in the projects approved by the Italian Ministero della Salute, Ufficio VI (authorization number 1060/2015 PR) and were in compliance with the National Institutes of Health Guidelines for Use and Care of Laboratory Animals and with the 1964 Declaration of Helsinki and its later amendments. To generate constitutive muscle-specific FGF21 knockout animals, mice bearing FGF21 floxed alleles ($FGF21^{f/f}$) (The Jackson Laboratory) were crossed with transgenic mice expressing Cre under the control of a Myosin Light Chain 1 fast promoter.[23] Cre-negative littermates were used as controls. For starvation experiments, fed mice had free access to food and water while food pellets were removed for starved mice. Adult mice (3 to 5 months old) of the same sex, age, and body weight were fasted or stayed in fed condition for different time periods: 24 h for gene expression analysis, autophagy flux, and puromycin experiments; 48 h for wet muscle weight, cross-sectional area (CSA), and muscle force measurements. To identify the FGF21 deletion in skeletal muscle, genomic DNA was isolated from gastrocnemius (GNM) muscles of $FGF21^{f/f}$ and $FGF21^{-/-}$ mice. Two primer sets were used. Set 1 consists of one primer upstream the 5′ loxP site and the other primer inside FGF21 sequence, amplifying a 675 bp sequence corresponding to not deleted DNA (Fw: 5′-GAAGATCCCAACCT CCTCCAG-3′, Rv: 5′-TGTCTTGGGTCGTCATCTGTGTA-3′). Set 2 detects muscle deletion of FGF21, consists of a couple of primers upstream 5′ loxP and downstream 3′ loxP sites detecting the deleted sequence in muscles of 300 bp (Fw: 5′-GAAGATCCCAACCTCCTCCAG-3′, Rv: 5′ACCGTGAATCCCAGCA CTA-3′). Mice were sacrificed by cervical dislocation, and the different tissues were weighed and then frozen in liquid nitrogen and utilized for histological experiments, immunohistochemistry, or gene expression studies.

Gene expression analyses

At least four samples of each experimental condition ($FGF21^{f/f}$ FED, $FGF21^{f/f}$ STARVED, $FGF21^{-/-}$ FED, and $FGF21^{f/f}$ STARVED) were analysed. Total RNA was prepared from GNM muscles using TRIzol (Life Technologies) following the manufacturer's instructions. Complementary DNA was generated from 400 ng of RNA reverse-transcribed with SuperScript IV Reverse Transcriptase (Life Technologies) according to manufacturer's instructions. At the end of the reaction, the volume of each samples was adjusted to 50 μL with RNase free water. Duplicates of cDNA samples were then amplified on the 7900HT Fast Real-Time PCR System (Applied Biosystems) using the PowerUp SYBR Green Master Mix (Applied Biosystems) following manufacturer's instructions. The PCR cycle used for qPCR was—step 1: 50°C 2 min; step 2: 95°C 2 min; step 3: 40 times of 95°C 15 s and 60°C 1 min; step 4: 95°C 15 s, 60°C 1 min and 95°C 15 s. No primer-dimers

were generated during qPCR amplification cycles. To avoid the amplification of genomic DNA, primer pair sequences were designed with Primer-Blast software (https://www.ncbi.nlm.nih.gov/tools/primer-blast/) on spanning exons, separated by a long intron, more than 1000 bp when possible. A dilution series of pooled cDNA was used to construct calibration curves. The slope of the log-linear portion of calibration curves for each primer was used to established primer PCR amplification efficacy. The oligonucleotide primers used are shown in Supporting Information, *Table* S1. The relative expression ratio of target gene was calculated based on PCR efficiency and quantification cycle deviation (Cq) of unknown sample vs. control and expressed in comparison with reference gene. All data were normalized to the reference gene GAPDH expression, whose abundance did not change under all experimental conditions, and plotted in arbitrary units as mean ± SEM. For FGF21 amplification, cDNA synthesis was obtained from 1.5 μg of RNA. FGF21 quantification was performed using TaqMan® Universal PCR Master Mix and the specific. TaqMan primers FGF21 (Mm 00840165_g1, Life Technologies). Data were normalized to GAPDH expression (Mm 99999915_g1, Life Technologies). Results are expressed as mean ± SEM.

Immunohistochemistry and stainings

Cryosections of adult GNM cross-sections were stained for haematoxylin and eosin (H&E), periodic acid–Schiff (PAS), and succinate dehydrogenase (SDH). CSA and fibre typing were calculated from entire muscle cross-section based on assembled mosaic image (×20 magnification). For fibre typing, slides were incubated using the following monoclonal antibody combination: BA-D5 (1:100) (Developmental Studies Hybridoma Bank) that recognizes type 1 MyHC isoform, SC-71 (1:100) (Developmental Studies Hybridoma Bank) for the type 2A MyHC isoform, and anti-dystrophin (1:100) (ab15277, Abcam, Cambridge, VK) for the sarcolemma. The images were captured using a Leica DFC300-FX digital charge-coupled device camera and the Leica DC Viewer software. The morphometric analyses were made using MATLAB Semi-Automatic Muscle Analysis using Segmentation of Histology software.

Force measurements

In vivo GNM force measurements were performed as described previously.[24] Briefly, mice were anaesthetized, and stainless-steel electrodes wires were placed on either side of the sciatic nerve. Torque production of the plantar flexors was measured using a muscle lever system (Model 305c; Aurora Scientific, Aurora ON, Canada). The force–frequency curves were determined by increasing the stimulation frequency in a stepwise manner, pausing for 30 s between stimuli to avoid effects due to fatigue. Following force measurements, animals were sacrificed by cervical dislocation, and muscles were dissected and weighted. Force was normalized to the muscle mass as an estimate of specific force.

Immunoblotting

Muscles were lysed and immunoblotted as previously described.[25] Blots were stripped using Restore Western Blotting Stripping Buffer (Pierce) according to the manufacturer's instructions and reprobed if necessary. The membranes were visualized with the ImageQuant LAS 4000 and quantified using ImageJ software (https://imagej.nih.gov/ij/). Protein expression was normalized to actin or GAPDH. List of antibodies is depicted in Supporting Information, *Table* S2.

Mitochondrial isolation

Mitochondria from quadriceps muscles of the indicated genotypes were isolated as described[18] and were then probed with the indicated antibodies by immunoblotting.

Autophagic flux quantification

Autophagic flux was monitored in both fed and 24 h of starvation conditions using colchicine (Sigma-Aldrich Chemie, C9754).[26] Briefly, mice were treated with 0.4 mg/kg of colchicine or vehicle by intraperitoneal injection. The treatment was administered twice, at 24 h and at 12 h, before muscle dissection. Total muscle and mitochondrial homogenates were used to measured autophagy and mitophagy flux, respectively.

Mito-mKeima mitophagy assay

Electroporation experiments were performed on flexor digitorum brevis (FDB) muscles from wildtype and knockout animals. The animals were anaesthetized by an intraperitoneal injection of xylazine (Xilor) (20 mg/kg) and Zoletil (10 mg/kg); 7 μL of hyaluronidase (2 mg/mL) (Sigma-Aldrich) were injected in the feet of anaesthetized mice to soften muscle tissue underneath the epidermis. After 50 min, 10 μg of mitochondria-targeted mKeima plasmid (mt-mKeima) were injected, and after 10 min, electric pulses were applied by two stainless needles placed at 1 cm from each other (100 V/cm) (100 Volts/cm, 20 pulses, 1 s intervals). Muscles were analysed 12 days later. FDB muscles were collected in 1% P/S DMEM. FDBs were digested in type I collagenase at 37°C for 1.5–2 h. The fibres were dissociated by creating mechanical forces using a pipette. The single isolated fibres were

then plated on glass coverslips coated with 10% Matrigel in Tyrode's salt solution (pH 7.4) and incubated overnight at 37°C. mt-mKeima (MBL International) was used to monitor mitophagy in transfected FDB single fibres. mt-mKeima is a coral-derived protein that exhibits both pH-dependent excitation and resistance to lysosomal proteases. These properties allow rapid determinations to whether the protein is in mitochondria or in the lysosome.[27,28] In fluorescence microscopy, ionized Keima is detected as a red fluorescent signal at pH 4 (lysosome) and as a green fluorescent signal at pH 7 (autophagosome).[29] Fluorescence of mt-mKeima was imaged in two channels via two sequential excitations (458 nm, green; 561 nm, red) and using a 570–695 nm emission range. The level of mitophagy was defined as the total number of red pixels divided by the total number of green pixels.

In vivo protein synthesis measurements

In vivo protein synthesis was measured by using the surface sensing of translation technique.[30,31] Mice were anaesthetized and then given an intraperitoneal injection of 0.040 μmol/g puromycin dissolved in 100 μL of phosphate buffered saline. At exactly 30 min after injection, muscles were collected and frozen in liquid N2 for western blot analysis. A mouse IgG2a monoclonal anti-puromycin antibody (clone 12D10, 1:5000) was used to detect puromycin incorporation.

Fibroblast growth factor 21 overexpression

For the cloning mouse *Fgf21* gene, muscle cDNA was amplified by PCR using the primers forward: 3′-TCAAGCTTTCA GGACGCATAGCTG-5′ and reverse: 3′ATGCTAGGATGGAATG GATGAGATCTAGA-5′. The amplified sequence was cloned into pBI-CMV1-GFP (PT4440-5, Clontech Laboratories, US/CA) expression vector and sequenced by GATC Biotech (Konstanz, Germany).

In vivo transfection experiments

Mice were co-transfected with mCherry-LC3 combined with either pBI-CMV1-GFP-FGF21 or pBI-CMV1-GFP. *In vivo* RNAi experiments were performed using pSuper-Bnip3 plasmid, which was already validated earlier both *in vitro* and *in vivo*.[25] *In vivo* transfection of tibialis anterior (TA) muscle was carried out using the NEPA21 Super Electroporator with settings: 21 voltage, 20 ms pulse length, 200 ms pulse internal, total five pulses. At least five mice were electroporated. The right TA muscle was electroporated with mCherry-LC3 and the control vectors pBI-CMV1-GFP or pSuper-mock vector while the left muscle was electroporated with mCherry-LC3 and pBI-CMV1-GFP-FGF21 and/or pSuper-Bnip3 plasmids. Muscles were collected 12 days after transfection.

LC3-vesicles quantification

Cryosections of wild type muscles that were transfected *in vivo* with mCherry–LC3 together with either CMV1-GFP-FGF21 GFP-FGF21 or with pBI-CMV1-GFP were examined using an epifluorescence Leica DM5000B microscope equipped with a Leica DFC300-FX digital charge-coupled device camera by using Leica DC Viewer software. The fluorescent dots were counted and normalized for cross-sectional area with ImageJ software.

Statistical analysis

All data are presented as mean ± SEM. Statistical analysis from two experimental groups ($Fgf21^{f/f}$ compared with $Fgf21^{-/-}$) was performed using unpaired one-tailed or two-tailed Student's *t*-tests. Comparisons of data from more than two groups were performed using a two-way analysis of variance. When analysis of variance revealed significant differences, further analysis was performed using Bonferroni's multiple comparison test. The statistical significance threshold was set at $P < 0.05$. *Significant to $Fgf21^{f/f}$ FED, $^{\#}$Significant to $Fgf21^{-/-}$ FED, $^{\S}Fgf21^{f/f}$ STARVED significant to $Fgf21^{-/-}$ STARVED, and $Fgf21^{f/f}$ FED significant to $Fgf21^{-/-}$ FED.

Results

Fibroblast growth factor 21 is dispensable for muscle mass maintenance in basal conditions

The metabolic regulator FGF21 is expressed and released into the general circulation by several tissues such as the liver, WAT, BAT, and the heart.[7–11] Recent studies reported that skeletal muscle is not only a producer but also a target of FGF21 because it expresses the cofactor β-klotho and the FGFRs.[6,13,14,17–19] However, the physiological role of FGF21 in skeletal muscle function has not been investigated yet. For this reason, we generated muscle-specific FGF21 knockout mice. FGF21 floxed mice ($FGF21^{f/f}$) were crossed with a transgenic line expressing Cre recombinase under the control of muscle-specific MLC1f promoter, which starts to be expressed during embryogenesis.[23] The resulting FGF21 muscle-specific knockout mice (hereafter referred to as $FGF21^{-/-}$) were born at the expected Mendelian ratio, were viable, and had a normal growth curve compared with age-matched control littermates ($FGF21^{f/f}$) (Supporting Information, *Figure* S1). The effective ablation of the floxed sequence from genomic DNA extracted from skeletal muscle

was confirmed by PCR analysis (*Figure* 1A). Quantitative real-time PCR (q-PCR) also revealed the efficient reduction of FGF21 transcript levels (*Figure* 1B). To assess the role of FGF21 in skeletal muscle homeostasis in resting conditions, we performed histological analysis of muscles of both control and FGF21$^{-/-}$ adult mice. H&E staining of transverse muscle sections detected a normal muscle architecture with no signs of inflammation, degeneration, or regeneration (central nucleated fibres) in FGF21 null muscles (*Figure* 1C). The distribution of glycogen stores revealed by PAS staining was unaffected by FGF21 deletion (*Figure* 1C). The wet weight of TA, GNM, extensor digitorum longus, and soleus hindlimb muscles was similar to controls (Supporting Information, *Figure* S2A). Quantitative analysis of myosin heavy chain distribution (*Figure* 1D) and of fibre size measurements of GNM muscles (*Figure* 1E and *Figure* 1F) did not show any difference between control and FGF21 knockout mice. These results indicate that FGF21 does not contribute

Figure 1 Muscle-specific FGF21 deletion does not affect muscle size or histology. (A) Genotyping of FGF21 control and knockout mice. PCR analysis with genomic DNA from gastrocnemius muscles. Two sets of primers were used. Set 1 consists of one primer upstream of the 5′ loxP site and the other primer inside FGF21 sequence, amplifying a 675 bp sequence corresponding to not deleted DNA; set 2 consists of a couple of primers upstream 5′ loxP and downstream 3′ loxP sites that detects the deleted sequence. (B) FGF21 mRNA expression was quantified by q-PCR in tibialis anterior muscle of FGF21$^{-/-}$ and control mice. (C) Representative H&E and PAS staining showing normal morphology, and glycogen content of FGF21$^{-/-}$ gastrocnemius muscle. (D) Percentage of fibres expressing myosin heavy chain types I, IIA, IIB, and IIX proteins in gastrocnemius muscles revealed by immunohistochemistry analysis. (E) Quantification of CSA of myofibers indicates no significant differences in FGF21-ablated muscles. (F) Frequency histograms showing the distribution of cross-sectional areas (μm^2) in GNM of FGF21$^{f/f}$ (black dashed line) and FGF21$^{-/-}$ (black line) fibres. Data are shown as mean ± SEM. $^{*}P < 0.05$. CSA, cross-sectional area; FGF21, fibroblast growth factor 21; H&E, haematoxylin and eosin; PAS, periodic acid–Schiff.

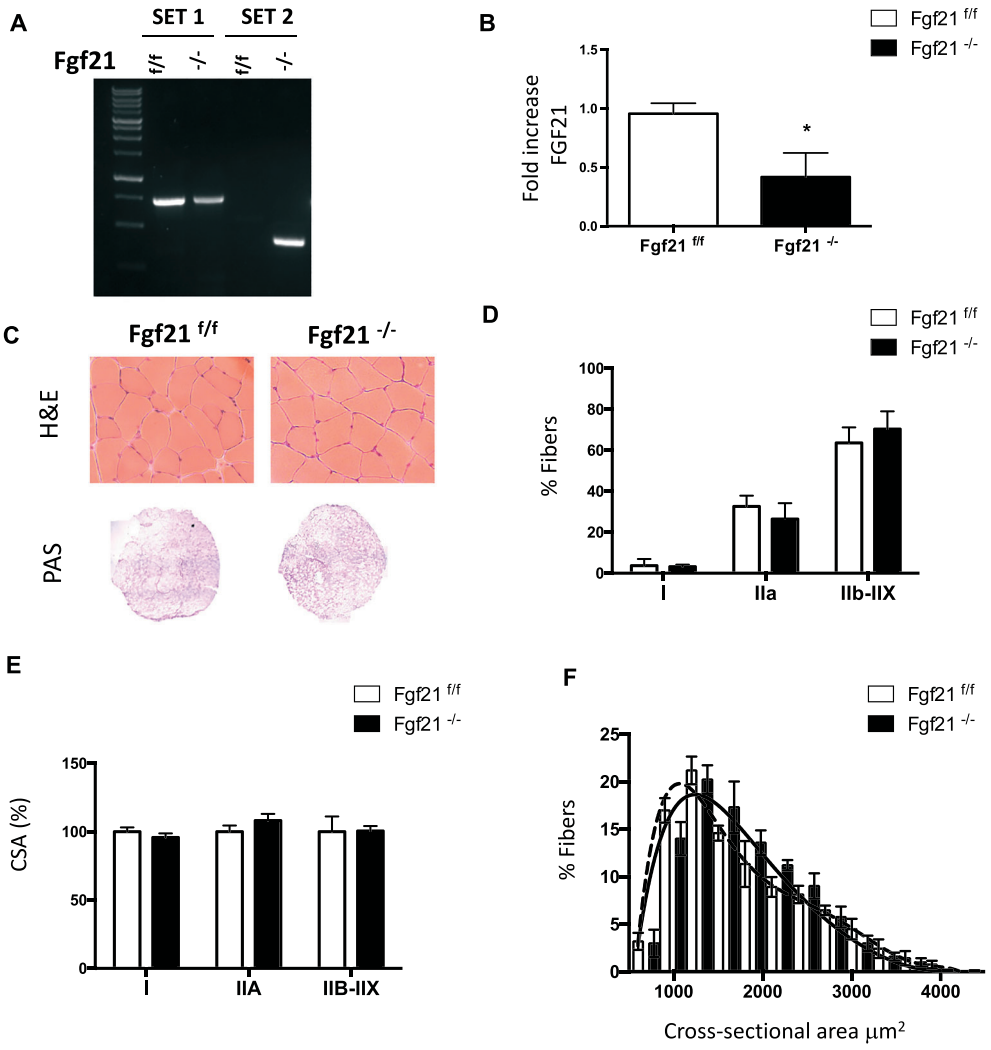

DOI: 10.1002/jcsm.12409

to muscle homeostasis in basal conditions, in terms neither of fibre type nor of fibre size.

Muscle-specific fibroblast growth factor 21 deletion protects against starvation-induced muscle atrophy and weakness

Under normal physiological conditions, expression levels of FGF21 in muscle are very low. In contrast, stress situations such as ER stress or mitochondrial myopathies induce FGF21 production in muscles.[13,14,17,18] Starvation is one of the stress conditions known to induce FGF21 expression in the liver,[8,32] WAT,[10] and skeletal muscle (*Figure* 2A).[6] The binding of the fasting-induced protein FGF21 relies on membrane-bound co-receptor β-Klotho to establish the activation of the receptor FGFR. FGF21 mainly binds to FGFR1 (FGFR1b and FGFR1c) and to a lower extent to FGFR4.[33] Accordingly, the expression of the FGF21 receptors: FGFR1, 1b, and 1c but not FGFR4 increase in muscles during starvation (Supporting Information, *Figure* S2B). Of note, in FGF21-null mice during fasting, FGFR1c is slightly lower while β-Klotho expression is significantly reduced (Supporting Information, *Figure* S2B). The metabolic adaptation mediated by FGF21 during fasting in the liver and WAT is known to increase lipolysis and hepatic ketogenesis.[34] However, the exact role of muscle-derived FGF21 in skeletal muscle during fasting is unknown. To determine the effects of FGF21 in adult skeletal muscles, we analysed the consequences in muscle function of the muscle-specific deletion of FGF21 after 48 h of fasting, which is both a model of metabolic stress and of muscle wasting. Muscle histology analyses by H&E staining of both controls and FGF21 knockout-fasted mice showed normal structure (*Figure* 2B), as seen in fed mice (*Figure* 1C). PAS staining showed increased glycogen content and thereby energy storage in knockout animals vs. control during starvation (*Figure* 2C). Remarkably, quantification of cross-sectional area of GNM muscles after prolonged fasting resulted in near 20% decrease in control muscles while FGF21 knockout mice were completely protected from muscle loss in terms of both cross-sectional area mean and fibre size distribution (*Figure* 2D and 2E). Fibre size of fasted knockout muscles was significantly higher in IIX-IIB fibres (*Figure* 2F) while fibre type composition, based on myosin heavy chain distribution, was unaffected (Supporting Information, *Figure* S2C). Interestingly, the observed protection against atrophy occurs not only in GNM muscles but also in other muscles with different metabolic properties and fibre type composition such as soleus (slow-oxidative fibres), extensor digitorum longus, and TA (predominance of type IIB fast-glycolytic fibres) (Supporting Information, *Figure* S2A). Consistent with muscle weight protection during fasting, the epididymal fat pads were also spared in knockout mice during fasting (Supporting Information, *Figure* S2D). To investigate if muscle mass sparing correlates with a functional protection, we measured the force generated by GNM muscle in living animals. As expected, control-fasted mice were significantly weaker than fed ones (*Figure* 2G). In contrast, in FGF21-deficient mice, absolute muscle force in fed and starved animals was almost superimposable (*Figure* 2H). When we analysed the force normalized for muscle mass, named specific force, no significant differences were detected in any of the conditions studied, indicating that there is no myopathy in the absence of FGF21 (Supporting Information, *Figure* S2E). Altogether, these results suggest that increased expression of FGF21 during fasting is required for muscle atrophy and weakness.

Protein synthesis rate is maintained in fibroblast growth factor 21-null muscles during fasting

The regulation of muscle size, due to its limited proliferative capacity, is determined by the co-ordinated balance between protein synthesis and protein degradation of myofibrillar components. Therefore, to explain the sparing in muscle mass and force with fasting, we hypothesized the possibility that FGF21 controlled either of the two processes. To assess the rate of new protein synthesis, we used the *in vivo* surface sensing of translation technique.[30] The antibiotic puromycin was injected intraperitoneally in control and knockout mice, and the rate of protein synthesis of nascent peptide chains that incorporated puromycin was analysed in GNM muscle by western blotting using an anti-puromycin antibody. In line with the results in muscle weight and CSA in fed conditions (Supporting Information, *Figure* S2A; *Figure* 1E and 1F), no significant differences in protein synthesis rate was observed in FGF21 knockout mice compared with controls (*Figure* 3A). Food deprivation, as expected, decreased protein synthesis rate of almost 70% in control muscles.[35] In contrast, in the absence of nutrients, protein synthesis rate of knockout mice was similar to that in knockout fed (*Figure* 3A). Because muscle loss requires the activation of transcription-dependent programme controlled by the regulation of a subset of genes named atrophy-related genes or atrogenes,[36] we monitored several atrogenes mRNAs belonging to ubiquitin-proteasome system (UPS).[37] The expression levels of the well-known muscle-specific E3 ubiquitin ligases Atrogin1 and MuRF1, as well as the recently discovered SMART, MUSA1, Fbxo31, Itch, and Trim37,[37] were the same in control and knockout muscles in both fed and fasting state (Supporting Information, *Figure* S3A). We checked the levels of Lys48 and Lys63 polyubiquitinated proteins, which play a role in the proteasomal-dependent and autophagy-dependent degradation, respectively (*Figure* 3B; *Figure* 3C; and Supporting Information, *Figure* S3B and S3C). As expected, fasting resulted in an increase of both Lys48 and Lys63 polyubiquitinated proteins in control mice. In contrast, in fasted FGF21-null

DOI: 10.1002/jcsm.12409

Figure 2 FGF21 is required for muscle atrophy and weakness during fasting. (A) mRNA expression of FGF21 in GNM of fed and starved FGF21$^{f/f}$ mice. (B) H&E staining of control (FGF21$^{f/f}$) and KO mice (FGF21$^{-/-}$) GNM muscle. (C) PAS staining shows more glycogen content in FGF21 null muscles. (D) Cross-sectional area of fed and 48 h starved GNM muscles. (E) Fibre size distribution from fed (left panel) and starved (right panel) control (black dashed line) and FGF21 KO (red line) muscles. (F) CSA of myofibers expressing myosin heavy chain types IIA and IIB-IIX of starved control and KO mice. (G) Force measurements performed *in vivo* on gastrocnemius showed that FGF21$^{-/-}$ muscles preserve muscle force after fasting. Force/frequency curve of FGF21$^{f/f}$ (left panel) and FGF21$^{-/-}$ (right panel). Data are shown as mean ± SEM. Significance $P < 0.05$ *vs. control fed, §vs. control starved. CSA, cross-sectional area; FGF21, fibroblast growth factor 21; H&E, haematoxylin and eosin; KO, knockout; PAS, periodic acid–Schiff.

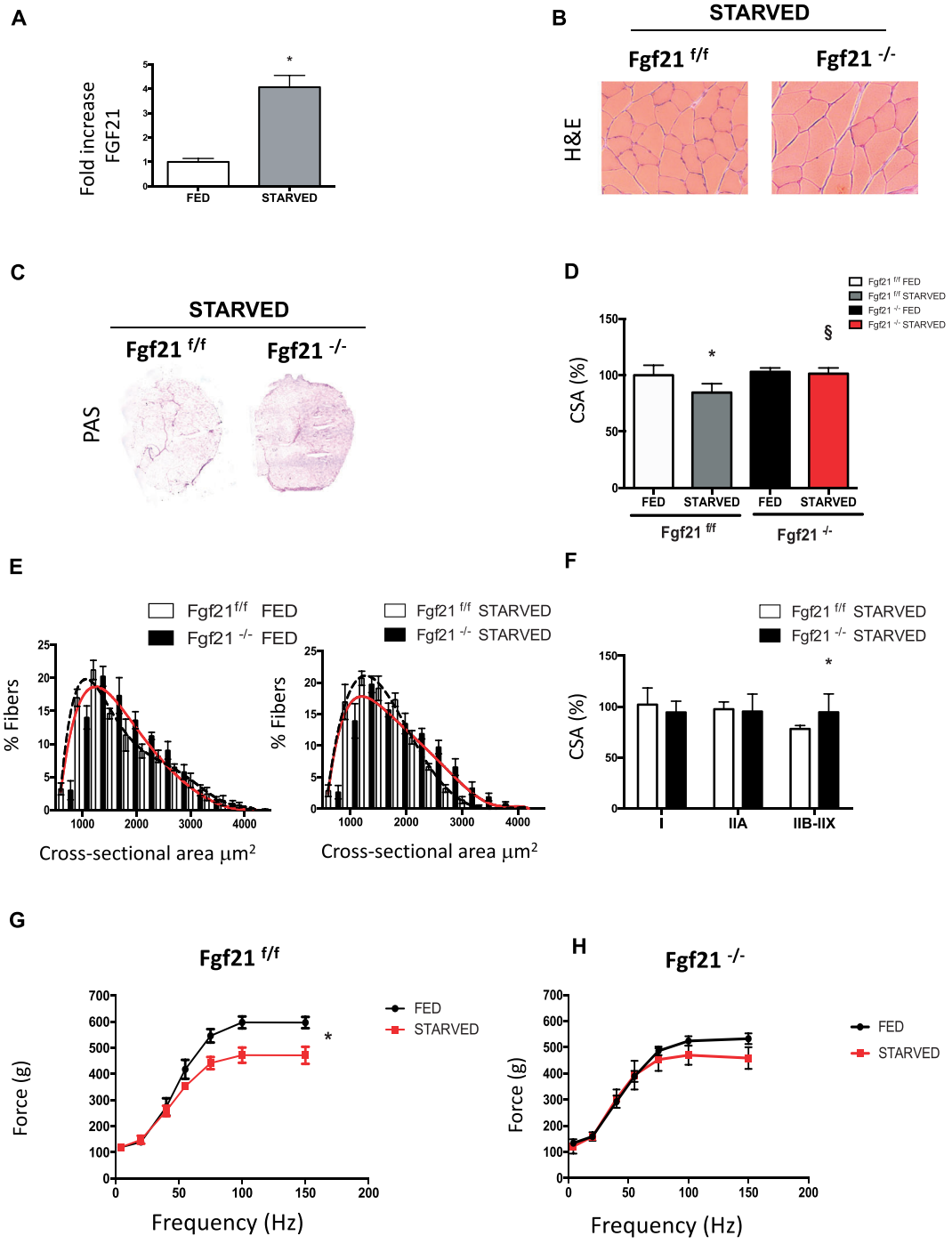

DOI: 10.1002/jcsm.12409

Figure 3 Protein synthesis rate is maintained in FGF21-deleted muscles during fasting. (A) *In vivo* surface sensing of translation technique shows the maintenance of protein synthesis in FGF21-ablated mice muscles during fasting. A representative immunoblot is shown. Quantification of the puromycin-labelled peptides is expressed as percentage of the values obtained in the control group. Data are normalized to actin. (B–C) Densitometric analysis of total muscle extracts from $FGF21^{f/f}$ and $FGF21^{-/-}$immunoblotted for anti-ubiquitin (Lys48) (B) and for anti-ubiquitin (Lys63) (C) normalized to actin. Data are shown as mean ± SEM. Protein bands were quantified using ImageJ, normalized to actin, and their expression was plotted relative to control fed (set to 1.00). Significance: *compared with control fed ($P < 0.01$), and compared with control fed ($P < 0.05$), #compared to FGF21 knockout fed ($P < 0.05$) and §vs. control starved ($P < 0.05$). FGF21, fibroblast growth factor 21.

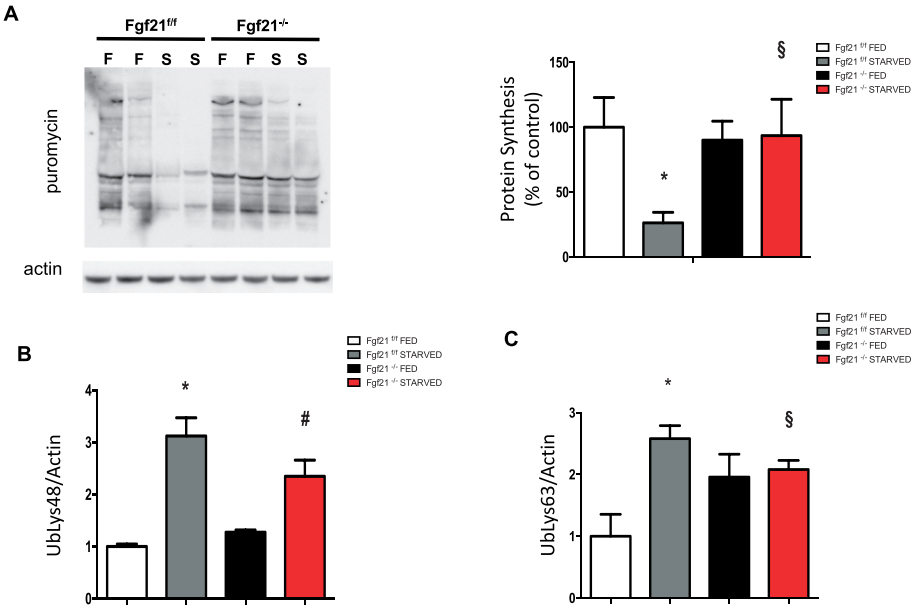

muscles, the accumulation of ubiquitin (Lys63) was lower comparing knockout with control mice while there were no significant differences in ubiquitin (Lys48) expression (*Figure* 3B, *Figure* 3C, and Supporting Information, *Figure* S3B and S3C). Collectively, these results suggest that in the absence of nutrients, the protection from fasting-induced muscle loss in FGF21 null muscles depend on the maintenance of protein synthesis rate together with a reduction of the autophagy-dependent degradation while the UPS activation is not altered.

Fibroblast growth factor 21 controls muscle mitophagy flux

Because the UPS was not involved in muscle mass and force sparing in fasted FGF21-null mice, we focused in the other muscle major degradative pathway, the autophagy lysosomal system, which is essential for muscle homeostasis.[38,39] The decrease of ubiquitin (Lys63) suggests that autophagy might be affected in Fgf21-null mice under starvation, as ubiquitin (Lys63) is important in the recognition of autophagy cargo (*Figure* 3C and Supporting Information, *Figure* S3C). However, no significant differences were observed in the transcript levels of several autophagy-related genes (Supporting Information, *Figure* S4A). Thus, the next step was to assess autophagic flux, *in vivo*, by using the autophagy-inhibiting drug colchicine, to block autophagosome maturation to autolysosomes. When blocking autophagic flux, the accumulation of LC3-II reflects autophagosome synthesis in the absence of degradation. Autophagic flux in total muscle homogenates remained unchanged in fed, suggesting that basal-general autophagic flux was not altered (*Figure* 4A and 4C left panel and Supporting Information, *Figure* S4B). As expected, colchicine treatment in fasted control mice caused a significant increase of LC3II levels during fasting, indicating that autophagy was ongoing in these muscles. In contrast, the general autophagy flux was partially reduced in starved condition in Fgf21-deleted mice (*Figure* 4A and 4C right panel and Supporting Information, *Figure* S4B). Because mitophagy, the selective degradation of dysfunctional mitochondria, is critical for the maintenance of muscle mass,[2] we isolated mitochondria from muscles treated with colchicine to evaluate the autophagy-dependent lysosomal delivery of mitochondria, named mitophagy. Interestingly, the autophagic flux of the mitochondrial fraction was significantly decreased in both fed and starved conditions in knockout mice (*Figure* 4D, 4E, and 4F and Supporting Information, *Figure* S4C). Additional evidence for the reduction of the mitophagy flux during fasting in FGF21 knockout mice was supported by time-lapse analyses of transfected adult muscles with the pH-sensitive mitochondrial target protein mt-

DOI: 10.1002/jcsm.12409

Figure 4 Muscle-specific FGF21 deletion controls mitophagy. Immunoblotting analyses of autophagy flux in control and FGF21-null GNM total muscle homogenates in fed (A) and in fasting (B) conditions. (C) Quantification of LC3 lipidation was normalized to actin and plotted to control fed not treated with colchicine (set to 1.00). Inhibition of autophagy–lysosome fusion by colchicine treatment induces less accumulation of LC3II band in starved FGF21-KO but not in starved control muscles. Mitophagy flux is decreased in FGF21 KO muscles. (D–E) Representative immunoblot images of mitochondria isolated from GNM muscles after colchicine treatment probed with anti-LC3 antibody in fed (D) and in fasting conditions. (F) Quantification of protein bands as seen in (D and E) by ImageJ. VDAC served as a loading control. (G) Mitophagy flux was analysed by electroporation of a reporter plasmid (mt-mKEIMA) into flexor digitorum brevis muscles of adult control and FGF21$^{-/-}$mice; changes of fluorescent spectra were detected and normalized to fibre area. (H) Succinate dehydrogenase staining indicating more mitochondrial content in FGF21 KO GNM muscles in both fed and fasting. (I) Mitochondrial content revealed by Tom20 is increased in FGF21-deleted muscles during fasting. Densitometric quantification of Tom20 western blot, normalized to GAPDH. (J) The mitophagy protein Bnip3 is significantly reduced in KO muscles. Densitometric analysis of Bnip3 protein, normalized to the mitochondrial protein VDAC and plotted relative to control fed. Data are shown as mean ± SEM. Significance $P < 0.05$ *compared with control fed and compared with control fed and §compared with control starved. FGF21, fibroblast growth factor 21; GNM, gastrocnemius; KO, knockout.

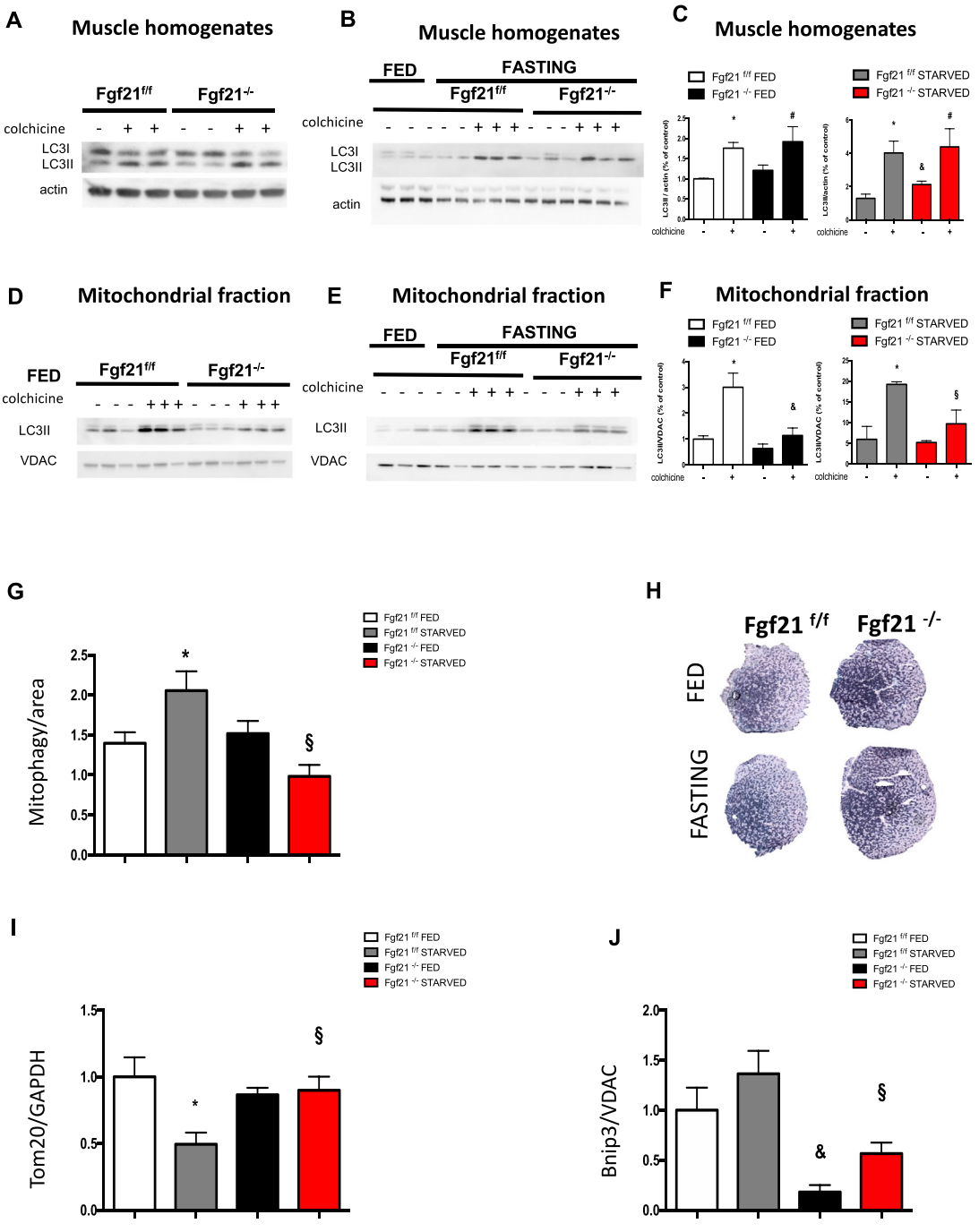

DOI: 10.1002/jcsm.12409

mKeima[27] (*Figure* 4G). Although mt-mKeima was not able to reveal differences in the basal mitophagy flux between knockout and control muscles, mitochondrial content, revealed by SDH staining, was higher in both fed and fasting FGF21-null muscles when compared with controls (*Figure* 4H). The reduction of mitophagy flux in the absence of FGF21 was further confirmed by significant increase in mitochondrial mass, revealed by Tom20 immunoblot (*Figure* 4I and Supporting Information, *Figure* S4D) and by decreased levels of the mitophagy protein Bnip3 (*Figure* 4J and Supporting Information, *Figure* S4E). In summary, FGF21 controls more specifically the mitophagic flux rather than the general autophagy, which was partially reduced in knockout mice during fasting.

Bnip3 is required for fibroblast growth factor 21-mediated muscle loss

To further address the contribution of FGF21 to the atrophy programme, we co-transfected, *in vivo*, TA adult muscles with mcherry-LC3 and with either a bidirectional plasmid encoding FGF21 and green fluorescent protein (GFP) or only GFP (mock plasmid) (*Figure* 5A). Twelve days after

Figure 5 *In vivo* overexpression of FGF21 in muscles induces autophagy and Bnip3-dependent muscle atrophy. (A–B) FGF21 overexpression induces autophagy. (A) Representative images of adult tibialis anterior muscles of wild type mice electroporated *in vivo* with mcherry-LC3 and with either GFP-FGF21 or with only GFP (control). Muscles were collected 12 days after transfection. (B) A higher number of LC3 dots was observed in muscles overexpressing FGF21. Quantification of the number of LC3 positive vesicles normalized to fibre area in control or in FGF21 overexpressing muscles. (C) FGF21 *in vivo* overexpression is sufficient to induce muscle loss. CSA of transfected fibres, identified by GFP immunofluorescence, was measured with ImageJ and normalized to control fibres. (D) Frequency histograms showing the distribution of cross-sectional areas (μm^2) in tibialis anterior transfected with either a GFP-plasmid (control) (black dashed line) or with GFP-FGF21 plasmid (red line). (E) Downregulation of Bnip3, by RNAi protects from FGF21-dependent muscle loss. Adult skeletal muscles were co-transfected with either GFP or with FGF21 in the presence or absence of specific siRNAs for mouse Bnip3. Twelve days later, muscles were collected and analysed for CSA of transfected fibres. Data are shown as mean ± SEM. $^{*}P < 0.05$. CSA, cross-sectional area; FGF21, fibroblast growth factor 21; GFP, green fluorescent protein.

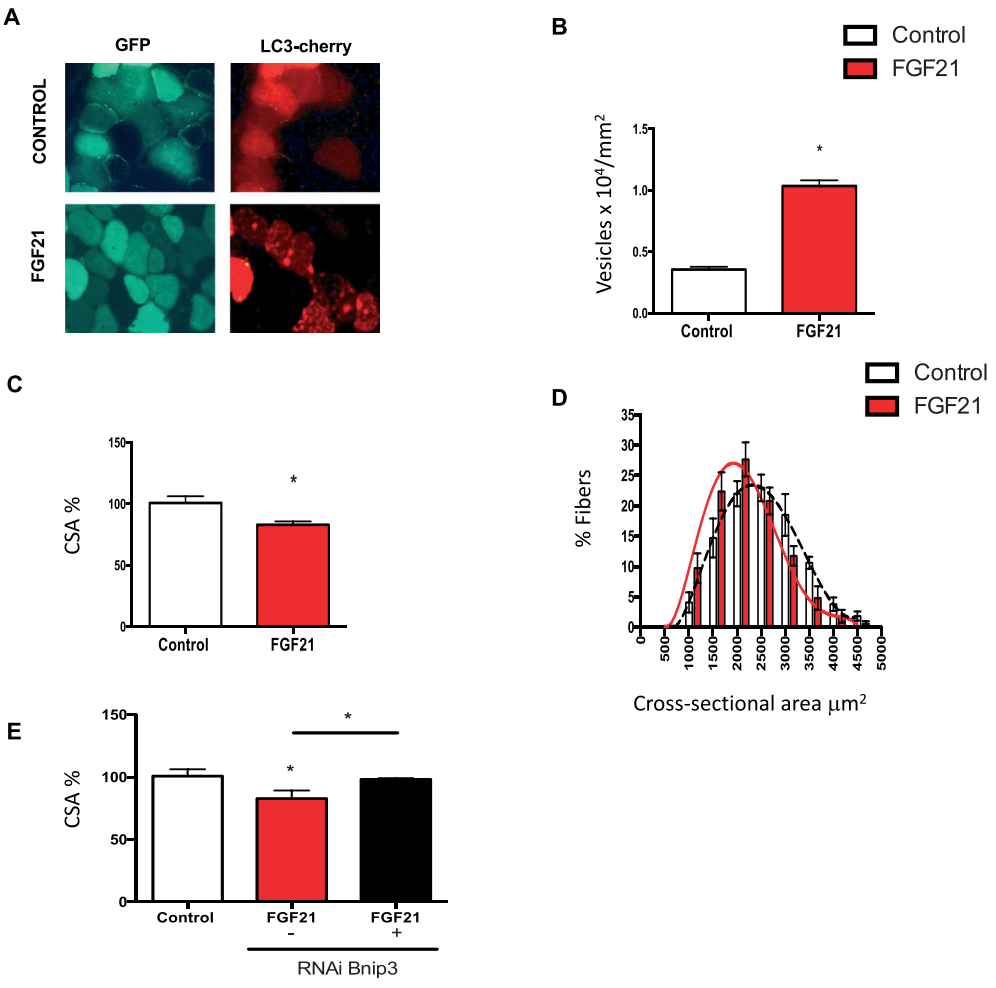

DOI: 10.1002/jcsm.12409

transfection, autophagosome formation was analysed by quantifying LC3-positive autophagic vesicles. Interestingly, autophagosome quantification was significantly higher in FGF21-expressing fibres than in mock-transfected fibres (*Figure* 5B). Because FGF21 is required for atrophy during prolongued fasting, we then investigated whether FGF21 overexpression was sufficient to induce muscle atrophy. Transfection of the mock vector does not alter myofiber size (*Figure* 5C). In contrast, FGF21 overexpression results in approximately 15% decrease in cross-sectional area of transfected fibres compared with the surrounding non-transfected fibres (*Figure* 5C). Accordingly, fibre size distribution shifted towards a smaller fibre size (*Figure* 5D). Because the levels of the mitophagy protein Bnip3 were significantly reduced in isolated mitochondria from FGF21-deleted muscles (*Figure* 4J and Supporting Information, *Figure* S4E) and we already demonstrated that Bnip3 inhibition reduces autophagosome formation and protects against muscle loss during atrophy,[25,38] we hypothesize an involvement of this factor in FGF21-mediated atrophy. We co-transfected, *in vivo*, vectors producing double-stranded small interfering RNA (siRNA) specific for Bnip3 together with FGF21-GFP plasmid. Inhibition of Bnip3 resulted in a significant protection from FGF21-induced muscle loss (*Figure* 5E), suggesting that Bnip3 is required for FGF21-dependent muscle atrophy.

Discussion

Here, we identify FGF21 as a novel player in the regulation of muscle mass. Moreover, our data provide insights into the mechanisms regulated by FGF21. Whether FGF21 is beneficial or detrimental for human health is so far still under debate. On one hand, FGF21 has gained attention for being a potential therapeutic protein for obesity and type 2 diabetes because it stimulates the oxidation of fatty acids, the production of ketone bodies, and inhibits lipogenesis.[33,34] On the other hand, several reports indicate a pathophysiological role for FGF21: (i) it promotes bone loss and reduces bone mineral density[40,41]; (ii) FGF21 is a stress-induced myokine, which is released under conditions of starvation, ER stress, mitochondrial dysfunction, obesity, mitochondrial myopathies, and aging.[6,13–18] We have recently shown that chronic elevation of muscle-derived circulating FGF21 leads to systemic inflammation, precocious senescence, and premature death.[18] Indeed, serum FGF21 levels positively correlated with aging sarcopenia.[18,21] Moreover, FGF21 is a specific serum biomarker of muscle-manifesting mitochondrial disorders[17,20] and for subclinical atherosclerosis,[42] and (iii) there is a paradoxically positive correlation with elevated serum FGF21 levels and metabolic disorders like obesity, diabetes, and mitochondrial diseases in mice and humans.[33] Interestingly, all these conditions have in common muscle atrophy. In fact, there is a tight correlation between muscle dysfunction and the disruption of physiological homeostasis at the whole body level. Therefore, the metabolic adaptations occurring in skeletal muscles can influence disease progression in distant tissues.[3,43] This regulation is exerted through the release of muscle-derived factors: myokines and myometabolites that can act systemically, in an endocrine fashion, to modulate the intertissue communication or locally in autocrine/paracrine manner. However, all the studies regarding FGF21 as a myokine revealed the endocrine signalling of FGF21, while the liver, WAT, BAT, and heart were shown to be both source and target of FGF21's autocrine/paracrine action.[34] Therefore, that muscle-derived FGF21 systemic contribution occur in stressed muscles is strongly supported.[6,13–18] What is not clear is which is the functional role of FGF21 in the context of skeletal muscle homeostasis. To clarify this issue, we explored in both fed and fasting conditions whether specific deletion of FGF21 in skeletal muscle affects the maintenance of adult skeletal muscle mass and the metabolic properties. In fed condition, loss of FGF21 in skeletal muscle does not induce any change in muscle mass, force, and fibre type, which is in agreement with low FGF21 expression levels under physiological conditions.[34] In contrast, FGF21 and FGFRs gene expression levels increase in muscles in response to fasting in control muscles. For this reason, we analysed whether the contribution of FGF21 to muscle function becomes evident in the absence of nutrients. Our data indicate that FGF21 is required for fasting-dependent muscle mass and force loss. Muscle mass and force sparing during fasting in knockout mice can be explained by the maintenance of protein synthesis rate. The increased protein synthesis without acting on protein breakdown may not be sufficient to prevent muscle atrophy and weakness during starvation, because the co-ordination of these two processes determines protein turnover. Our findings indicate that muscle protection in fasted FGF21 knockout mice does not depend on the regulation of UPS, but it rather depends on the regulation of autophagy and, more specifically, mitophagy pathways. Mitophagy flux is reduced in FGF21-null mice during fasting. Indeed, *in vivo* mt-mKeima experiment, SDH staining, and western blotting for the mitochondrial marker Tom20 and the mitochondrial degradation protein Bnip3 suggest that mitophagy is decreased. *In vivo* overexpression of FGF21 in skeletal muscle fibres is sufficient to significantly induce autophagosome formation and muscle loss, resulting in 15% of decrease of cross-sectional area of transfected TA fibres, supporting a role for FGF21 in skeletal muscle remodelling. Inhibition of the mitophagy factor Bnip3, *in vivo*, by RNAi, was sufficient to reduce FGF21-dependent muscle atrophy. Thus, Bnip3 is a key factor in muscle loss induced by FGF21. To our knowledge, this is the first study demonstrating that, in mammalian skeletal

muscle, FGF21 is involved in the removal of damaged mitochondria through mitophagy. In summary, the current study elucidates by using gain and loss of function approaches, a novel role for FGF21 in the control of skeletal muscle mass through the regulation of the anabolic/catabolic balance. These findings are important for the understanding of the molecular pathways that control muscle mass. Moreover, this study also open several new avenues for future investigation to define the mechanisms mediated by FGF21 in the interplay between muscle and other tissues such as bones, heart, and WAT in whole body homeostasis.

Acknowledgements

We are grateful to Dr. Asushi Miyawaki for the kind gift of mt-mKeima. This study was supported by Starting Grants CARIPARO to V.R. and AFM Research grant 21865 to B.B. The authors certify that they comply with the ethical guidelines for publishing in the *Journal of Cachexia, Sarcopenia and Muscle: update 2017*.[44]

Online supplementary material

Additional supporting information may be found online in the Supporting Information section at the end of the article.

Table S1: Sequences of primers used for Quantitative Real Time Analysis
Table S2: List of primary antibodies used for Western Blotting in this study
Figure S1: Body weight of both, females (upper graph) and males (lower graph) versus post-natal weeks of control and FGF21-null mice.
Figure S2: A) Wet weight relative to control of Tibialis anterior (TA), Gastrocnemius (GNM), Extensor Digitorum Longus (EDL) and Soleus muscles of controls and KO mice in fed and after 48 h of fasting B) RT-PCR for β-klotho (KLB) and different FGF receptors isoforms in skeletal muscle of fed and fasted control and FGF21 KO mice C) % of fibers expressing myosin heavy chain type I, IIA, IIB and IIX proteins in gastrocnemius muscles revealed by immunohistochemistry analysis in starved control and FGF21-null mice D) Epididymal fat content normalized to body weight (BW) is preserved in FGF21 KO mice during fasting E) Absolute muscle force normalized to GNM wet weight indicates the absence of myopathy in the conditions analyzed. Significance $p< 0.05$. * compared to control fed, & compared to control fed, #compared to FGF21 KO fed, and § versus control starved.
Figure S3: A) q–PCR of Ubiquitin-Proteasome System-related transcripts from fed and 24-h starved tibialis anterior of control and FGF21 -/- muscles. Data are normalized to GAPDH and expressed as fold increase of control-fed mice B and C) Representative Western Blots of total muscle extracts immunoblotted for anti-Ubiquitin (Lys48) (B) and for anti-Ubiquitin (Lys63) (C) normalized to actin. Data are shown as mean ± s.e.m. Significance $p< 0.05$. * compared to control fed, & compared to control fed, #compared to FGF21 KO fed and § versus control starved.
Figure S4: A) q-PCR analysis of autophagy-related transcripts in fed and starved control and KO muscles normalized to GAPDH B) Fold increase of LC3II western blot of total muscle homogenates normalized to actin and plotted as a ratio between colchicine treated samples and paired samples without colchicine C) Fold increase of LC3II western blot of the mitochondrial fraction normalized to VDAC and plotted as a ratio between colchicine treated samples and paired samples without colchicine D) Representative Western Blots of Tom20 in muscle homogenates (D) and of Bnip3 in the mitochondrial fraction (E). Data are shown as mean ± s.e.m. Significance $p< 0.05$. * compared to control fed, & compared to control fed, #compared to FGF21 KO fed and § versus control starved.

Conflict of interest

None declared.

References

1. Volaklis KA, Halle M, Meisinger C. Muscular strength as a strong predictor of mortality: a narrative review. *Eur J Intern Med* 2015;**26**:303–310.
2. Romanello V, Sandri M. Mitochondrial quality control and muscle mass maintenance. *Front Physiol* 2015;**6**:422.
3. Rai M, Demontis F. Systemic nutrient and stress signaling via myokines and myometabolites. *Annu Rev Physiol* 2016;**78**:85–107.
4. Whitham M, Febbraio MA. The ever-expanding myokinome: discovery challenges and therapeutic implications. *Nat Rev Drug Discov* 2016;**15**:719–729.
5. Pedersen BK, Steensberg A, Fischer C, Keller C, Keller P, Plomgaard P, et al. Searching for the exercise factor: is IL-6 a candidate? *J Muscle Res Cell Motil* 2003;**24**:113–119.
6. Izumiya Y, Bina HA, Ouchi N, Akasaki Y, Kharitonenkov A, Walsh K. FGF21 is an Akt-regulated myokine. *FEBS Lett* 2008;**582**:3805–3810.
7. Badman MK, Pissios P, Kennedy AR, Koukos G, Flier JS, Maratos-Flier E. Hepatic fibroblast growth factor 21 is regulated by PPARα and is a key mediator of hepatic lipid metabolism in ketotic states. *Cell Metab* 2007;**5**:426–437.
8. Inagaki T, Dutchak P, Zhao G, Ding X, Gautron L, Parameswara V, et al. Endocrine regulation of the fasting response by

PPARα-mediated induction of fibroblast growth factor 21. *Cell Metab* 2007;**5**:415–425.
9. Patel V, Adya R, Chen J, Ramanjaneya M, Bari MF, Bhudia SK, et al. Novel insights into the cardio-protective effects of FGF21 in lean and obese rat hearts. *PLoS One* 2014;**9**:e87102.
10. Muise ES, Azzolina B, Kuo DW, El-Sherbeini M, Tan Y, Yuan X, et al. Adipose fibroblast growth factor 21 is up-regulated by peroxisome proliferator-activated receptor gamma and altered metabolic states. *Mol Pharmacol* 2008;**74**:403–412.
11. Hondares E, Iglesias R, Giralt A, Gonzalez FJ, Giralt M, Mampel T, et al. Thermogenic activation induces FGF21 expression and release in brown adipose tissue. *J Biol Chem* 2011;**286**:12983–12990.
12. Markan KR, Naber MC, Ameka MK, Anderegg MD, Mangelsdorf DJ, Kliewer SA, et al. Circulating FGF21 is liver derived and enhances glucose uptake during refeeding and overfeeding. *Diabetes* 2014;**63**:4057–4063.
13. Keipert S, Ost M, Johann K, Imber F, Jastroch M, van Schothorst EM, et al. Skeletal muscle mitochondrial uncoupling drives endocrine cross-talk through the induction of FGF21 as a myokine. *Am J Physiol Endocrinol Metab* 2014;**306**:E469–E482.
14. Ost M, Coleman V, Voigt A, van Schothorst EM, Keipert S, van der Stelt I, et al. Muscle mitochondrial stress adaptation operates independently of endogenous FGF21 action. *Mol Metab* 2016;**5**:79–90.
15. Pereira RO, Tadinada SM, Zasadny FM, Oliveira KJ, Pires KMP, Olvera A, et al. OPA1 deficiency promotes secretion of FGF21 from muscle that prevents obesity and insulin resistance. *EMBO J* 2017;**36**:2126–2145.
16. Rodriguez-Nuevo A, Diaz-Ramos A, Noguera E, Diaz-Saez F, Duran X, Munoz JP, et al. Mitochondrial DNA and TLR9 drive muscle inflammation upon Opa1 deficiency. *EMBO J* 2018;**37**:e96553.
17. Suomalainen A, Elo JM, Pietilainen KH, Hakonen AH, Sevastianova K, Korpela M, et al. FGF-21 as a biomarker for muscle-manifesting mitochondrial respiratory chain deficiencies: a diagnostic study. *Lancet Neurol* 2011;**10**:806–818.
18. Tezze C, Romanello V, Desbats MA, Fadini GP, Albiero M, Favaro G, et al. Age-associated loss of OPA1 in muscle impacts muscle mass, metabolic homeostasis, systemic inflammation, *and Epithelial Senescence*. *Cell Metab* 2017;**25**:1374–1389 e6.
19. Vandanmagsar B, Warfel JD, Wicks SE, Ghosh S, Salbaum JM, Burk D, et al. Impaired mitochondrial fat oxidation induces FGF21 in muscle. *Cell Rep* 2016;**15**:1686–1699.
20. Lehtonen JM, Forsstrom S, Bottani E, Viscomi C, Baris OR, Isoniemi H, et al. FGF21 is a biomarker for mitochondrial translation and mtDNA maintenance disorders. *Neurology* 2016;**87**:2290–2299.
21. Hanks LJ, Gutierrez OM, Bamman MM, Ashraf A, McCormick KL, Casazza K. et al. Circulating levels of fibroblast growth factor-21 increase with age independently of body composition indices among healthy individuals. *J Clin Transl Endocrinol* 2015;**2**:77–82.
22. Benoit B, Meugnier E, Castelli M, Chanon S, Vieille-Marchiset A, Durand C, et al. Fibroblast growth factor 19 regulates skeletal muscle mass and ameliorates muscle wasting in mice. *Nat Med* 2017;**23**:990–996.
23. Bothe GW, Haspel JA, Smith CL, Wiener HH, Burden SJ. Selective expression of Cre recombinase in skeletal muscle fibers. *Genesis* 2000;**26**:165–166.
24. Marabita M, Baraldo M, Solagna F, Ceelen JJM, Sartori R, Nolte H, et al. S6K1 is required for increasing skeletal muscle force during hypertrophy. *Cell Rep* 2016;**17**:501–513.
25. Romanello V, Guadagnin E, Gomes L, Roder I, Sandri C, Petersen Y, et al. Mitochondrial fission and remodelling contributes to muscle atrophy. *EMBO J* 2010;**29**:1774–1785.
26. Ju JS, Varadhachary AS, Miller SE, Weihl CC. Quantitation of "autophagic flux" in mature skeletal muscle. *Autophagy* 2010;**6**:929–935.
27. Katayama H, Kogure T, Mizushima N, Yoshimori T, Miyawaki A. A sensitive and quantitative technique for detecting autophagic events based on lysosomal delivery. *Chem Biol* 2011;**18**:1042–1052.
28. Sun N, Yun J, Liu J, Malide D, Liu C, Rovira II, et al. Measuring in vivo mitophagy. *Mol Cell* 2015;**60**:685–696.
29. Proikas-Cezanne T, Codogno P. A new fluorescence-based assay for autophagy. *Chem Biol* 2011;**18**:940–941.
30. Schmidt EK, Clavarino G, Ceppi M, Pierre P. SUnSET, a nonradioactive method to monitor protein synthesis. *Nat Methods* 2009;**6**:275–277.
31. Goodman CA, Mabrey DM, Frey JW, Miu MH, Schmidt EK, Pierre P, et al. Novel insights into the regulation of skeletal muscle protein synthesis as revealed by a new nonradioactive in vivo technique. *FASEB J* 2011;**25**:1028–1039.
32. Potthoff MJ, Inagaki T, Satapati S, Ding X, He T, Goetz R, et al. FGF21 induces PGC-1α and regulates carbohydrate and fatty acid metabolism during the adaptive starvation response. *Proc Natl Acad Sci U S A* 2009;**106**:10853–10858.
33. Staiger H, Keuper M, Berti L, Hrabe de Angelis M, Haring HU. Fibroblast growth factor 21-metabolic role in mice and men. *Endocr Rev* 2017;**38**:468–488.
34. Fisher FM, Maratos-Flier E. Understanding the physiology of FGF21. *Annu Rev Physiol* 2016;**78**:223–241.
35. Yuan CL, Sharma N, Gilge DA, Stanley WC, Li Y, Hatzoglou M, et al. Preserved protein synthesis in the heart in response to acute fasting and chronic food restriction despite reductions in liver and skeletal muscle. *Am J Physiol Endocrinol Metab* 2008;**295**:E216–E222.
36. Cohen S, Nathan JA, Goldberg AL. Muscle wasting in disease: molecular mechanisms and promising therapies. *Nat Rev Drug Discov* 2015;**14**:58–74.
37. Milan G, Romanello V, Pescatore F, Armani A, Paik JH, Frasson L, et al. Regulation of autophagy and the ubiquitin-proteasome system by the FoxO transcriptional network during muscle atrophy. *Nat Commun* 2015;**6**:6670.
38. Mammucari C, Milan G, Romanello V, Masiero E, Rudolf R, Del Piccolo P, et al. FoxO3 controls autophagy in skeletal muscle in vivo. *Cell Metab* 2007;**6**:458–471.
39. Masiero E, Agatea L, Mammucari C, Blaauw B, Loro E, Komatsu M, et al. Autophagy is required to maintain muscle mass. *Cell Metab* 2009;**10**:507–515.
40. Fazeli PK, Faje AT, Cross EJ, Lee H, Rosen CJ, Bouxsein ML, et al. Serum FGF-21 levels are associated with worsened radial trabecular bone microarchitecture and decreased radial bone strength in women with anorexia nervosa. *Bone* 2015;**77**:6–11.
41. Wei W, Dutchak PA, Wang X, Ding X, Wang X, Bookout AL, et al. Fibroblast growth factor 21 promotes bone loss by potentiating the effects of peroxisome proliferator-activated receptor gamma. *Proc Natl Acad Sci U S A* 2012;**109**:3143–3148.
42. Kokkinos J, Tang S, Rye KA, Ong KL. The role of fibroblast growth factor 21 in atherosclerosis. *Atherosclerosis* 2017;**257**:259–265.
43. Baskin KK, Winders BR, Olson EN. Muscle as a "mediator" of systemic metabolism. *Cell Metab* 2015;**21**:237–248.
44. von Haehling S, Morley JE, Coats AJS, Anker SD. Ethical guidelines for publishing in the *Journal of cachexia, sarcopenia and muscle: update 2017*. *J Cachexia Sarcopenia Muscle* 2017;**8**:1081–1083.